Estimation of Number of Targets Based on CNN Classifier for OFDM Radar Systems

Jae-Woong Choi [1], Jeong-Eun Oh [1], A-Min Jo [1] and Eui-Rim Jeong [2 +]
[1] Graduate Student, Dept. of Mobile Convergence and Engineering, Hanbat National University, Daejeon, Republic of Korea
[2+] Professor, Dept. of Artificial Intelligence Software, Hanbat National University, Daejeon, Republic of Korea

Article Info
Page Number: 555 – 564
Publication Issue:
Vol. 71 No. 3 (2022)

Article History
Article Received: *12 January 2022*
Revised: *25 February 2022*
Accepted: *20 April 2022*
Publication: *09 June 2022*

Abstract

This paper proposes a new convolutional neural network (CNN) for estimating the number of targets in orthogonal frequency division multiplexing (OFDM) radar systems. The transmitter of OFDM radar system receives the signal reflected on the target. Two-dimensional periodogram is obtained via 2D fast Fourier transform (FFT) from the reflected signal after removing the modulation effect. Two-dimensional periodogram is an input signal for the CNN classifier. CNN classifier estimates the number of targets. We propose two types of CNN models. One is 7-layer CNN model and the other is 4-layer CNN model. The maximum number of targets was set to 2, 4 and 8. According to the simulation, the accuracy is degraded as the number of targets increased. Comparing the proposed 7-layer model and 4-layer model, the detection accuracy of 7-layer is about 23.9% better than 4-layer. However, 4-layer has much lower complexity than 7-layer.

Keywords: OFDM, Radar, two-dimensional periodogram, Target estimation, CNN.

1. Introduction

Radar is a wireless target detection technique that shows high detection performance in any weather and environment, such as fog, heavy rain, and darkness (Jaroszweski and Mcnamara, 2014). As a result, it continues to develop and is used in many fields such as automobiles, military, bio, and submarine (Feng et al., 2018, Liu et al., 2003, Rahman et al., 2018, Kim et al., 2011). Radar transmits radio waves from the antennas and receives radio waves reflected from objects to determine whether they are fixed or moving objects via the strength, size, and shape of the received radio waves. If it is a moving object, the radar determines the distance and speed (Mahafza, 2017). Thus, radar is being used in various fields, causing the problem

[+] Corresponding author. Tel.: +82-42-821-1752; fax: +82-42-821-1595.
E-mail address: erjeong@hanbat.ac.kr.

of frequency depletion (Bruder, 2013). To solve this problem, the technique that combines communication and radar is attracting a lot of attention (Wang et al., 2012). The combination of communication and radar means using the same frequency band for the two purposes (Fink and Jonddral, 2015). Among various communication schemes, orthogonal frequency division multiplexing (OFDM) is a popular mobile communication technique because simple frequency-domain equalizer can compensate for the multi-path channel distortion (Sen and Nehorai, 2010). Therefore, the use of systems that combine OFDM and radar is increasing (Sturm, 2010, Kauffman et al., 2013).

Recently, deep learning is received a lot of attention (Jo et al., 2021). To solve the radar problem, a technique that applies deep learning is being researched a lot (Li et al., 2019, Meyer and Kuschk, 2019). Among deep learning techniques, object detection using convolutional neural network (CNN) is a popular method. A research was proposed to use 7-layer CNN model for target estimation by inputting the two-dimensional periodogram as an input of CNN (Choi, 2021). The two-dimensional periodogram can be generated by radar signal processing. This paper proposes another new 7-layer CNN model, and 4-layer CNN model with smaller parameters to estimate the number of targets with 2D periodogram. If model is small and light, it has the advantage of lowering complexity and increasing efficiency. The detection performance is compared when the maximum number of targets was set to 2, 4 and 8. According to the simulation results, the accuracy is degraded as the number of targets increased. Comparing the proposed 7-layer model and 4-layer model, the detection accuracy of 7-layer is about 23.9% better than 4-layer. However, 4-layer has much smaller complexity than 7-layer.

2. OFDM Radar

Figure 1 shows OFDM radar system model dealing with in this paper. In the transmitter side, data is modulated and converted from serial to parallel. The m-th generated signal vector is represented as $\boldsymbol{u}_m = [u_{0.m}, u_{1.m}, \cdots u_{N-1.m}]^T$ where N is FFT size and $u_{n.m}$ is a complex symbol generated by digital modulation. The vector signal $\boldsymbol{u}_m$ is converted into time domain signal through IFFT. The output of IFFT is denoted by $\boldsymbol{u'}_m = [u'_{0.m}, u'_{1.m}, \cdots u'_{N-1.m}]^T$. After converting signal from parallel to serial, the guard interval or cyclic prefix (CP)is inserted in front of the signal to prevent inter OFDM symbol interference. The signal with CP is denoted as $\boldsymbol{u''}_m = [u'_{N-L_c.m}, \cdots u'_{N-1.m}, u'_{0.m}, u'_{1.m}, \cdots u'_{N-1.m}]$ where L_c is the length of CP. Then, $\boldsymbol{u''}_m$ is transmitted via Tx antenna and the reflected or returned signal from the targets is received via Rx antenna. Received signal is denoted as $\boldsymbol{y''}_m = [y'_{N-L_c.m}, \cdots y_{N-1.m}, y'_{0.m}, y'_{1.m}, \cdots y'_{N-1.m}]$. $\boldsymbol{u''}_m$ and $\boldsymbol{y''}_m$ are not same because of the time delay, Doppler frequency and signal attenuation. After removing CP at $\boldsymbol{y''}_m$ and converting from serial to parallel, the signal becomes $\boldsymbol{y'}_m = [y'_{0.m}, y'_{1.m}, \cdots y'_{N-1.m}]^T$. Then, by taking FFT, $\boldsymbol{y'}_m$, frequency domain signal is obtained. The output of FFT can be written as $\boldsymbol{y}_m = [y_{0.m}, y_{1.m}, \cdots y_{N-1.m}]^T$. Identify the targets can be done by comparing $\boldsymbol{u}_m$ and $\boldsymbol{y}_m$. The same procedure is repeated for the consecutive received OFDM symbols and resulting signals are stacked up to form a two-dimensional signal.

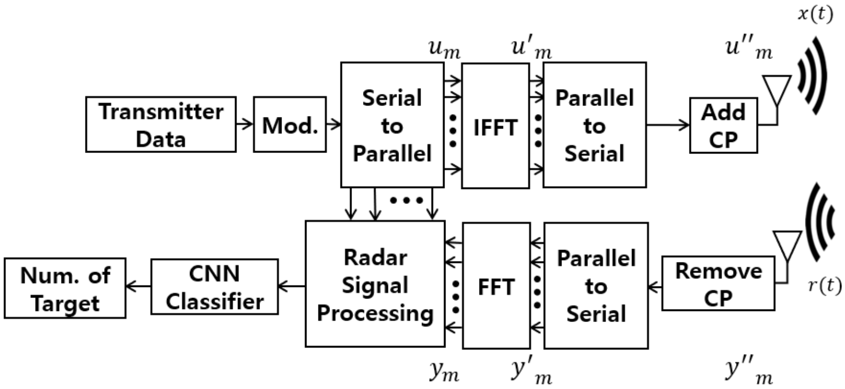

Fig. 1: OFDM radar system model

When total M OFDM symbols are transmitted, the transmitted signal matrix and received signal matrix can be represented as (1) and (2).

$$\boldsymbol{U} = \begin{pmatrix} u_{0,0} & u_{0,1} & \cdots & u_{0,M-1} \\ u_{1,0} & u_{1,1} & \cdots & u_{1,M-1} \\ \vdots & \vdots & \ddots & \vdots \\ u_{N-1,0} & u_{N-1,1} & \cdots & u_{N-1,M-1} \end{pmatrix} \tag{1}$$

$$\boldsymbol{Y_r} = \begin{pmatrix} y_{0,0} & y_{0,1} & \cdots & y_{0,M-1} \\ y_{1,0} & y_{1,1} & \cdots & y_{1,M-1} \\ \vdots & \vdots & \ddots & \vdots \\ y_{N-1,0} & y_{N-1,1} & \cdots & y_{N-1,M-1} \end{pmatrix} \tag{2}$$

In matrix (1) and (2), each row represents the subcarrier index while each column represents OFDM symbol index. For instance, $u_{5,2}$ represents the data of 6th subcarrier in 3th OFDM symbol. The following parameters are assumed to be known. The sampling frequency after the IFFT is f_S. The subcarrier space is $\Delta f(= f_S/N)$. Therefore, the OFDM symbol duration is $T(= 1/\Delta f)$. The duration of the CP is denoted by T_G. Thus, total duration of OFDM symbol is $T_O(= T + T_G)$. The center frequency is f_C.

To perform radar imaging and obtain two-dimensional periodogram, it transmits a signal $x(t)$ and receives a signal $r(t)$ at the same time. The signal $r(t)$ is composed of a superposition of reflections of the original signal on objects and receiver noise. In other words, while transmitting, the receiver picks up the reflected signal simultaneously. Thus, transmitter and receiver must be synchronized not to have any time or frequency offset. The received signal $r(t)$ has the form as

$$r(t) = \sum_{h=0}^{H_t-1} b_h x(t-\tau_h) e^{j2\pi f_{D,h} t} e^{j\phi_h} + \sum_{i=0}^{H_c-1} b_i x(t-\tau_i) e^{j\phi_i} + \tilde{\boldsymbol{Z}}(t) \tag{3}$$

where H_t is the number of reflecting targets and H_c is the number of clutter components. The time delay causes a phase shift of the individual elements $u_{k,l}$. The phase shift varies between subcarriers depending on its frequency. After combining these effects, $\boldsymbol{Y_r}$ becomes

$$(\boldsymbol{Y}_r)_{k,l} = \sum_{h=0}^{H_t-1} b_h (\boldsymbol{U})_{k,l} e^{j2\pi T_O f_{D,h} l} e^{-j2\pi\tau_h \Delta f k} e^{j\phi_h} + \sum_{i=0}^{H_c-1} b_i (\boldsymbol{U})_{k,l} e^{-j2\pi\tau_i \Delta f k} e^{j\phi_i} + (\widetilde{\boldsymbol{Z}})_{k,l} \tag{4}$$

where $(\boldsymbol{A})_{k.l}$ indicates the (k,l)-th element of matrix $\boldsymbol{A}$. The time delay is τ_h $(= 2 \times d_h/c_0)$ which is translated into distance d_h. Doppler frequency is $f_{D.h}(= 2 \times v_{rel.h}/c_0)$ where $v_{rel.h}$ and c_0 are relative velocity and the speed of light, respectively. The ϕ_h is an unknown phase offset and magnitude of the reflected signal b_h indicates signal attenuation and can be written as

$$b_h = \sqrt{\frac{c_0 \sigma_{RCS,h}}{(4\pi)^3 d_h^4 f_C^2}} \tag{5}$$

where $\sigma_{RCS.h}$ represents the size of the target. As mentioned earlier, clutter components make unwanted back-scattered signals by natural environments or coupling between Tx and Rx antenna. Therefore, equivalent distance and time delays of clutter components are close to zero, respectively. The distance of clutter component d_c is generated in the simulation by the Weibull distribution of probability density function.

$$f(d_c; \eta, \beta) = \frac{\beta}{\eta}\left(\frac{d_c}{\eta}\right)^{\beta-1} e^{-(d_c/\eta)^{\beta}} \tag{6}$$

where η and β are scale and shape parameters, respectively. The equivalent radar cross sections are randomly generated under uniform distribution. The matrix $\widetilde{\boldsymbol{Z}} \in C^{N\times M}$ is white Gaussian noise. To remove $\boldsymbol{U}$ in $\boldsymbol{Y}_r$, elements-wise division is performed to yield

$$(\boldsymbol{Y})_{k,l} \triangleq \frac{(\boldsymbol{Y}_r)_{k,l}}{(\boldsymbol{U})_{k,l}} = \sum_{h=0}^{H_t-1} b_h\, e^{j2\pi T_O f_{D,h} l} e^{-j2\pi\tau_h \Delta f k} e^{j\phi_h} + \sum_{i=0}^{H_c-1} b_i\, e^{-j2\pi\tau_i \Delta f k} e^{j\phi_i} + (\boldsymbol{Z})_{k,l} \tag{7}$$

where $(\boldsymbol{Z})_{k.l} = (\widetilde{\boldsymbol{Z}})_{k,l}/(\boldsymbol{U})_{k.l}$. In (7), first exponential inside the summation comprises Doppler frequency and the second exponential comprises the time delay. The radar problem is to detect and identify the frequencies of the two sinusoids. To estimate the sinusoids, two-dimensional periodogram is used and has the form as

$$(\boldsymbol{P})_{N,M} = \frac{1}{NM}\left|\sum_{k=0}^{N-1}\sum_{l=0}^{M-1} (\boldsymbol{Y})_{k,l} (\boldsymbol{W})_{k.l} e^{-j2\pi\left(\frac{kn}{N_{FFT}} + \frac{lm}{M_{FFT}}\right)}\right|^2 \tag{8}$$

where $\boldsymbol{P}$ is two-dimensional periodogram and has size $N_{FFT} \times M_{FFT}$. In (8), The result of the sum inside the modulus operator is called periodogram. $N_{FFT} \times M_{FFT}$ is the size of two dimensional DFT (discreate Fourier transform). If N_{FFT} and M_{FFT} are chosen as integer multiples of N and M, estimation resolution can be improved. $\boldsymbol{W}$ is a window given by

$$\boldsymbol{W} = \boldsymbol{w}_N \boldsymbol{w}_M^T, \boldsymbol{w}_N \in R^{N\times1}, \boldsymbol{w}_M \in R^{M\times1} \tag{9}$$

where $\boldsymbol{w}_N$ and $\boldsymbol{w}_M$ are one-dimensional window vectors, respectively. Among several known window functions, we employ the Hanning window. If maximum distance and Doppler frequency of targets are limited within certain bound, only a cropped area of periodogram $\boldsymbol{P}$ is enough for target detection. Identifying targets corresponds to detection of local maximum in the periodogram. If a peak is found at indices $(\hat{n}, \hat{m})$, the target distance and relative velocity can be given as

$$\hat{d} = \frac{c_0 \hat{n}}{2\Delta f N_{FFT}} \tag{10}$$

$$\hat{v} = \frac{c_0 \hat{m}}{2 f_C T M_{FFT}} \tag{11}$$

Owing to the OFDM symbol duration T and the subcarrier spacing Δf, maximum of unambiguous ranges and relative velocities is given as follows:

$$\left| d_{max} \right|\left| \frac{c_0}{2\Delta f} \right| \tag{12}$$

$$\left| v_{max} \right|\left| \frac{c_0}{2 f_C T_O} \right| \tag{13}$$

If Δf and T are designed to be small enough, the maximum unambiguous values can admit the available distance and velocity of targets.

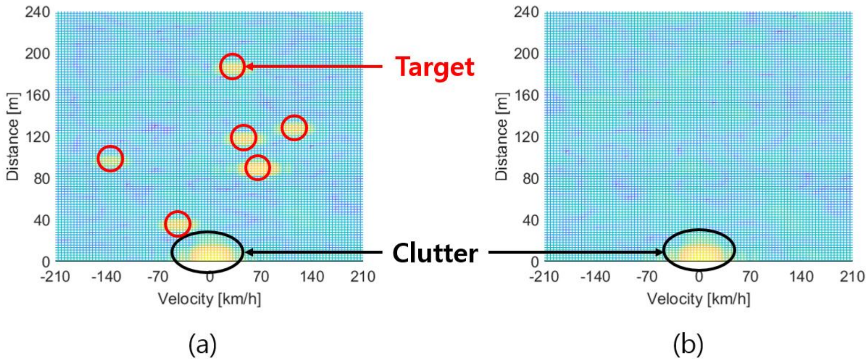

Fig. 2: Example of periodogram, $\boldsymbol{P}$, (a) target + clutter ('T+C') (b) clutter ('C')

Figure 2 shows an example of $\boldsymbol{P}$ when there are six targets. In Figure 2 (a) shows that target and clutter are together (‘T+C’), and (b) shows that target does not exist (‘C’). There are two input methods for CNN classifier. We will call the method of inputting only ‘T+C’ as single image input, and the method of inputting 'T+C' and 'C' together as dual image input. The clutter components such as stationary targets are observed with velocity 0. Positive and negative velocity imply approaching and leaving target, respectively.

3. Proposed CNN Model

CNN is a kind of deep learning models and is a useful technique for finding patterns in images. Finding targets in the periodogram can be regarded as an image detection problem. Thus, it is reasonable to solve radar problem using CNN. In this paper, the two types of CNN model are proposed. One is 7-layer CNN model ('L7 CNN') and the other is a 4-layer model ('L4 CNN').

The proposed L7 CNN structure is shown in Figure 3. L7 CNN consists of six convolutional layers, one fully connected layer, and one softmax layer. The size of the convolutional filter is 5x5 for all convolutional layers, and the channel size increases from 16 to 512 by a multiple of 2. The max pooling is performed after the first and second convolutional layers. Each convolutional layer has a batch normalization layer and ReLU layer. After, fully connected layer is performed. The final output of the fully connected layer is H_t+1. H_t is the maximum number of targets, and the possible classes are from 0 to H_t. The number of parameters is 4,690,241 + 320,001*H_t for a single image input, and 4,690,641 + 320,001* H_t for a dual image input.

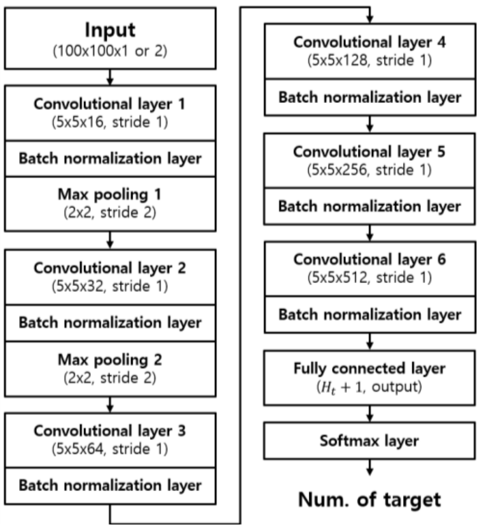

Fig. 3: Proposed L7 CNN

The proposed L4 CNN structure is shown in Figure 4. L4 CNN consists of three convolutional layers and one fully connected layer, and one softmax layer. The size of the convolutional filter is 3x3 for all convolutional layers, and the channel size increases from 32 to 128 by a multiple of 2. Each convolutional layer uses max pooling and has batch normalization layer and ReLU layer. After that, fully connected layer is performed. Finally, the output of the fully connected layer is H_t+1. The number of parameters is 173,539 + 80,001*H_t for a single image input, and 173,639 + 80,001*H_t for a dual image input.

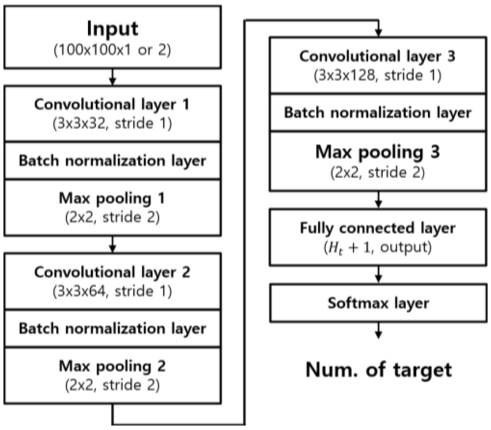

Fig. 4: Proposed L4 CNN

4. Simulation

4.1. Simulation environment

The performance of the proposed CNN model is conducted by computer simulation with Matlab and Tensorflow. Matlab is used to generate two-dimensional periodogram. two-dimensional periodogram is the input of CNN classifier. The parameters used to generate two-dimensional periodogram are summarized in Table 1. The sampling clock is 122.88MHz, the bandwidth is 40MHz, the center frequency is 40MHz, and the subcarrier space is 30kHz. The number of symbols is 64 and the length of CP is 296. 1284 subcarriers out of 4096 subcarriers are active. Finally, H_t uses 2, 4, and 8 to randomly generate the number of objects from 0 to 2, 4, and 8. The velocity and distance of generated object are also randomly generated among 7~240km/h and -190~190m, respectively.

Table 1: parameters of OFDM Radar

Parameter	Value
Sampling clock	122.88MHz
Bandwidth	40MHz
Center frequency	28GHz
Subcarrier space	30kHz
OFDM symbol	64
CP size	296
FFT point	1284 of 4096
H_t	2,4,8

Tensorflow is used for training and testing the CNN. The parameters for CNN are shown in Table 2. Both L7 CNN and L4 CNN use the same parameters. Training data is 110,000 and randomly generated from SNR = -14dB to 22dB. The test data is generated from SNR -20dB to 22dB with 3dB interval and 10,000 data are generated at each SNR. The minibatch size is 100 and the maximum epoch is 100. The optimizer is Adam with learning rate 0.001. The size of two-dimensional periodogram is 100x100x1 for single image input and 100x100x2 for dual image input. Finally, the cost function uses Cross Entropy Error, which is typically used in classification problems.

Table 2: parameters for CNN training

Parameter	Value
Num. of training data	110,000
Num. of test data	10,000
Minibatch size	100
Max epoch	100
Optimizer	Adam
Learning rate	0.001
Input size	100x100x1 100x100x2
Cost function	CEE

4.2. Result of CNN training

Figure 5 shows learning curve according to the maximum number of objects. Figure 5 (a) is the learning curve of the L7 CNN, and Figure 5 (b) is the learning curve of L4 CNN. In case of $H_t = 2$, it is lime green line and $H_t = 4$, violet line and $H_t = 8$, dodger blue line. In addition, the case of single image input is solid line, and the case of dual image input is dotted line. The L7 CNN is robust to the maximum number of objects, which converges close to 0 at the end of training. On the other hand, in L4 CNN, the loss is 0 to 0.2 at the end of training. That is, L4 CNN has higher loss than L7 CNN in all cases.

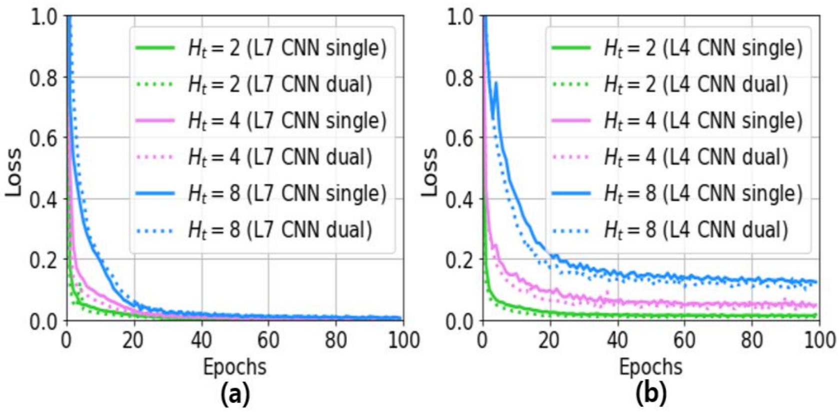

Fig. 5: Learning Curve, (a) L7 CNN, (b) L4 CNN

4.3. Performance comparison

Figure 6 is the object estimation accuracy. Figure 6 (a) is the object estimation accuracy of L7 CNN and Figure 6 (b) is the estimation accuracy of L4 CNN. Accuracy is calculated as

$$Accuracy = \frac{N_c}{N_t} * 100 \qquad (14)$$

where N_c is number of test data predicted correctly. N_t is the number of total test data. In case of $H_t = 2$, it is lime green line and circle marker and $H_t = 4$, violet line and square marker and $H_t = 8$, dodger blue line and triangle up marker. In addition, the case of single image input is presented solid line, and the case of dual image input is presented dotted line. Let's compare L7 CNN and L4 CNN at SNR 22dB. In a single image input, the accuracy when $H_t = 2$ and $H_t = 4$ is about 98.6% and about 98.6% for L7 CNN and about 99.2% and about 93.6% for L4 CNN. The difference is not much significant. However, when $H_t = 8$, L7 CNN is about 93.7% and L4 CNN is about 69.8%, which is a lot of difference. Also, in dual image input, the accuracy when $H_t = 2$ and $H_t = 4$ is about 99.3% and about 99.3% for L7 CNN and about 99.6% and 97.2% for L4 CNN, so the difference is not significant. However, when $H_t = 8$, L7 CNN is about 95.9% and L4 CNN is about 76.6%, which is a lot of difference. The proposed method has high accuracy as the SNR increases. In addition, when the input is dual, the accuracy is higher than that of single. And the accuracy decreases as the number of object estimation increases.

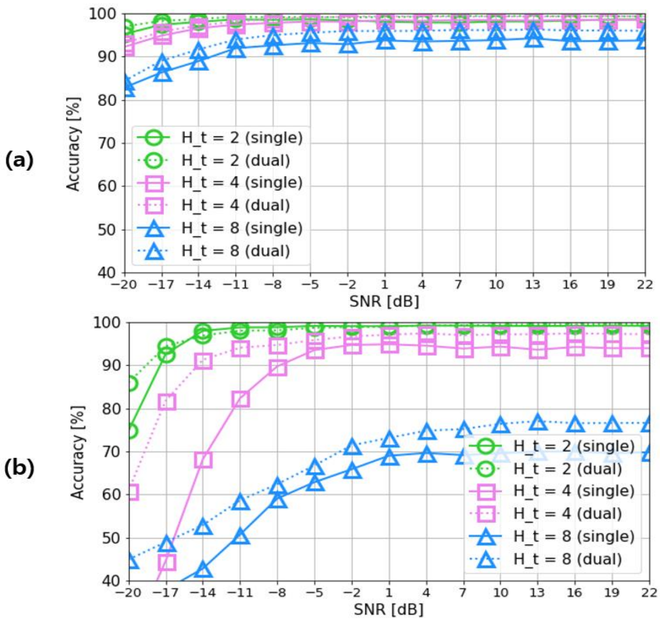

Fig. 6: Estimation accuracy performance. (a) L7 CNN, (b) L4 CNN

5. Conclusion

This paper proposed a CNN-based target estimation for OFDM radar systems. The proposed methods are L7 CNN and L4 CNN. Both proposed methods have higher performance than existing method. Comparing L7 CNN and L4 CNN, L7 CNN performance is better than L4 CNN overall. Though, the total number of parameters is 4,690,241 + 320,001*H_t or 4,690,641 + 320,001*H_t for L7 CNN, and 173,539 + 80,001*H_t or 173,639 + 80,001*H_t for L4 CNN. Therefore, the complexity of L4 CNN is about 19.6 times lower than that of L7 CNN.

6. Acknowledgements

This work was supported by Institute of Information & communications Technology Planning & Evaluation (IITP) grant funded by the Korea government (MSIT) (No.2018-0-01663, Development of Communication-Sensing Converged B5G Millimeter Wave System)

7. References

1. Bruder, J. A. (2013). IEEE Radar standards and the radar systems panel. *IEEE Aerospace and Electronic Systems Magazine*, 28(7), 19-22.
2. Choi, J. W. (2021). Multiple Target Detection for OFDM radar Based On Convolutional Neural Network. *Turkish Journal of Computer and Mathematics Education (TURCOMAT)*, 12(6), 544-550.
3. Feng, Z., Li, M., Stolz, M., Kunert, M. & Wiesbeck, W. (2018). Lane detection with a high-resolution automotive radar by introducing a new type of road marking. *IEEE Transactions on Intelligent Transportation Systems*, 20(7), 2430-2447.
4. Fink, J. & Jondral, F. K. (2015). Comparison of OFDM radar and chirp sequence radar. In *2015 16th International Radar Symposium (IRS)* (pp. 315-320). IEEE.
5. Jaroszweski, D. & McNamara, T. (2014). The influence of rainfall on road accidents in urban areas: A weather radar approach. *Travel behaviour and society*, 1(1), 15-21.
6. Jo, J. H., Bang, J. H., Yoo, I. H., Kim, T. H. & Sun, M. Y. (2021). A Deep learning Algorithm Design for the Classification the Shape of Molten Marks for the Cause Analysis of Electric Fires. *Journal of Next-generation Convergence Technology Association*, 5(6), 1011-1017.
7. Kauffman, K., Raquet, J., Morton, Y. & Garmatyuk, D. (2013). Real-time UWB-OFDM radar-based navigation in unknown terrain. *IEEE Transactions on Aerospace and Electronic Systems*, 49(3), 1453-1466.
8. Li, X., He, Y. & Jing, X. (2019). A survey of deep learning-based human activity recognition in radar. *Remote Sensing*, 11(9), 1068.
9. Liu, G. S., Gu, H., Su, W. M., Sun, H. B. & Zhang, J. H. (2003). Random signal radar-a winner in both the military and civilian operating environments. *IEEE Transactions on Aerospace and Electronic Systems*, 39(2), 489-498.
10. Mahafza, B. R. (2017). *Introduction to radar analysis*. Chapman and Hall/CRC.
11. Kim, D. J., Moon, W. M., Kim, G., Park, S. E. & Lee, H. (2011). Submarine groundwater discharge in tidal flats revealed by space-borne synthetic aperture radar. *Remote Sensing of Environment*, 115(2), 793-800.
12. Meyer, M. & Kuschk, G. (2019). Automotive radar dataset for deep learning based 3d object detection. In *2019 16th european radar conference (EuRAD)* (pp. 129-132). IEEE.
13. Sen, S. & Nehorai, A. (2010). Adaptive OFDM radar for target detection in multipath scenarios. *IEEE Transactions on Signal Processing*, 59(1), 78-90.
14. Rahman, A., Lubecke, V. M., Boric–Lubecke, O., Prins, J. H. & Sakamoto, T. (2018). Doppler radar techniques for accurate respiration characterization and subject identification. *IEEE Journal on Emerging and Selected Topics in Circuits and Systems*, 8(2), 350-359.
15. Sturm, C., Zwick, T., Wiesbeck, W., & Braun, M. (2010). Performance verification of symbol-based OFDM radar processing. In *2010 IEEE Radar Conference* (pp. 60-63). IEEE.
16. Wang, H., Wang, J. & Li, H. (2012). Target detection using CDMA based passive bistatic radar. *Journal of systems engineering and electronics*, 23(6), 858-865.